Atmospheric Environment 220 (2020) 117066

Contents lists available at ScienceDirect

Atmospheric Environment

journal homepage: http://www.elsevier.com/locate/atmosenv

A comprehensive analysis of the spatio-temporal variation of urban air pollution in China during 2014–2018

Hao Fan, Chuanfeng Zhao *, Yikun Yang

State Key Laboratory of Earth Surface Processes and Resource Ecology, College of Global Change and Earth System Science, Beijing Normal University, Beijing, 100875, China

HIGHLIGHTS

- 87%, 63% and 93% stations showed decreasing CO, NO_2 and SO_2 in recent 5 years.
- 78% and 89% stations showed decreasing PM_{10} and $PM_{2.5}$ in recent 5 years.
- The North China Plain and central-Western Xinjiang areas are the most seriously polluted.
- The improvement of air quality is associated with rigorous emission control in China.

ARTICLE INFO

Keywords:
Air pollution
Spatio-temporal analysis
Particulate matter
Emission control
China

ABSTRACT

Air pollution has been a serious environmental problem in China that damages human health and causes climate change. While air pollution has been extensively investigated, few studies have provided systematic research on the recent space-time changes in air pollution components, including the AQI, CO, O_3, NO_2, SO_2, PM_{10} and $PM_{2.5}$, over all of China. Based on the national air quality ground observation database, with data from more than 300 cities from May 2014 to December 2018, this study provides a comprehensive analysis of the characteristics and temporal trends of air pollution over the 7 classified regions in China. Compared to 2014, there are significant decreases of air pollutants in 2018, which are 16% AQI, 25% CO, 20% NO_2, 52% SO_2, 20% PM_{10}, and 28% $PM_{2.5}$. The constant improvement of air quality is mainly associated with rigorous emission control acts in China, along with the changes of meteorology. In contrast, O_3 maximum daily 8 h average (O_3MDA8) continuously increased at an average rate of 4.6% per year during the study period. The air pollution components demonstrate distinct differences in spatial distribution, with high values of CO in North China and Northwest China, NO_2 in North China and East China, PM_{10} in Northwest China, $PM_{2.5}$ in North China and Central China, and SO_2 in North China and Northeast China. Generally, air pollution is most serious in the North China Plain and in cities in central and western Xinjiang Province. Causes for these spatial distributions have been discussed from the perspective of emissions.

1. Introduction

Air pollution has been a global concern of the public, the government and the scientific community (Hadley et al., 2018; X.Y. Li et al., 2017). Northern Hemisphere mid-latitude regions, including Europe, America and Asia, are major areas of air quality research (X.Y. Wang et al., 2018). Air pollution can not only cause various kinds of diseases (Brauer et al., 2016; Cohen et al., 2017; Requia et al., 2017), but also influence weather and climate resulting in more extreme weather events, including flooding and drought (Herrera-Estrada et al., 2018; Y.J. Li et al., 2017; Rosenfeld et al., 2019; Tie et al., 2016; Zhao et al., 2018). Therefore, it becomes necessary for us to improve our understanding of the spatial and temporal variations of air pollutants, the influencing factors on air pollution, and the potential ecological and environmental impacts of air pollution.

Located in East Asia, with an area of approximately 9.6 million square kilometres, China has the largest population in the world, with the urban population of 813.47 million and the rural population of 576.61 million in 2017 over the mainland. Its gross domestic production (GDP) has reached 8271.17 billion yuan RMB, to which industrial

* Corresponding author.
E-mail address: czhao@bnu.edu.cn (C. Zhao).

https://doi.org/10.1016/j.atmosenv.2019.117066
Received 20 April 2019; Received in revised form 12 October 2019; Accepted 18 October 2019
Available online 24 October 2019
1352-2310/

production contributes 34% as the most significant contributing factor (http://www.stats.gov.cn/tjsj/ndsj/). Along with the rapid development of the economy, air pollution has had a substantial influence on each sector of society for a long time.

The strong emissions have had serious adverse impacts in China (Y.J. Li et al., 2017; Zhao et al., 2019; Zhou and Zhou, 2017). Many studies have indicated that people exposed to polluted air are more susceptible to respiratory and cardiovascular diseases (Ebenstein et al., 2017; Hadley et al., 2018). In the typical high pollution cities of North China, the number of people hospitalized for hypertension increased by 0.56%, 0.31%, 1.18%, 0.40% and 0.03%, respectively, when the mass concentration of $PM_{2.5}$, PM_{10}, NO_2, O_3 and CO increased by 10 $\mu g\,m^{-3}$ (Song et al., 2019). $PM_{2.5}$ and PM_{10} denote air particles with dynamic diameters less than 2.5 µm and 10 µm, respectively. Air pollution has caused serious damages to the service, lives and health of China's working population, which is worth a total of 346,260 million yuan RMB (Xia et al., 2016). Moreover, air pollution particles can reduce atmospheric visibility and downwelling solar radiation directly (X.Y. Li et al., 2017).

Based on remote sensing and ground observation data, many studies have investigated the air quality in China in highly polluted areas, typical cities and city clusters (Shi et al., 2018; K.Y. Zhang et al., 2019; Zhang et al., 2016; Zhao et al., 2019; Zhong et al., 2018). For example, the concentration of $PM_{2.5}$ in Beijing exceeded the health standard recommended by the World Health Organization (WHO) dramatically in 2013 (Guan et al., 2014). As indicated by Liu et al. (2019), the annual average $PM_{2.5}$ mass concentrations monitored in 74 major cities in 2013 and 2015, respectively, are 2.1 and 1.4 times higher than the grade 2 maximum allowable mass concentration value (35 $\mu g\,m^{-3}$) required by the National Ambient Air Quality Standard of China (NAAQS, GB 3095–2012) and are more than 5 times higher than the maximum allowable mass concentration value (10 $\mu g\,m^{-3}$) recommended by the WHO Air Quality Guidelines. In contrast, there are relatively insufficient studies about the air quality over the whole country. As indicated by previous studies, meteorological conditions (e.g., rainfall, humidity, and wind speed), terrain conditions, natural emissions, and human activity-based emissions are the most important factors affecting air quality (Kang et al., 2019; Tian et al., 2019). In addition to the most polluted cities, which mainly lie in North and Central China, studies of the air pollution over other regions in China are also important for understanding both the emission and the transport of air pollutants along with their impacts on local environments. While there are a large number of studies about the characteristics of $PM_{2.5}$, few studies have focused on pollution components other than $PM_{2.5}$, including SO_2, NO_2 and O_3, which also play an important role on air pollution in China (K. Li et al., 2019; R. Li et al., 2019; Zheng et al., 2018). It is therefore necessary for us to carry out a comprehensive air quality research on multiple contaminants to better understand the country's current air pollution status.

The China government not only issued several emission control policies in succession, but also set pollution abatement targets for provinces and certain cities according to their actual situation in recent years (Guan et al., 2014; Silver et al., 2018; Xia et al., 2016). In particular, the government has made many efforts to reduce industrial and vehicle exhaust emissions and to use clean energy, and all existing coal power plants have reached the requirements of the new emission standard (GB13223-2011) published on 1st July 2014 (Karplus et al., 2018). More and more rural areas have adopted relatively clean energy in their daily life and production in order to reduce air pollutants emissions (Karplus et al., 2018; Silver et al., 2018). In addition to working hard on emission reduction policies and emission reduction technologies, the China government has gradually strengthened air quality monitoring and network construction. Since January 2013, the Ministry of Environmental Protection of China has released real-time air quality and pollutant monitoring data. By 2014, 190 cities have joined the air quality data sharing services, which are located in every province in mainland China (K. Li et al., 2019; Zheng et al., 2018). The improvement of monitoring facilities and the expansion of monitoring coverage makes it possible to study the space-time features of air pollution in the country.

With great achievements in air quality control, the concentration and distribution pattern of air pollutants have changed during recent years in China. The $PM_{2.5}$ mass concentration in major cities clustered in East China has been a dramatic reduction (Silver et al., 2018; T. Wang et al., 2018). However, there has also been a rapid increase in the ozone concentration in those cities. By removing the influences of meteorological variables on the O_3 concentration, a multiple linear regression model analysis showed a distinct increase in the ozone concentration at a rate of 1–3 ppbv per year in major cities clustered in East China (K. Li et al., 2019). A comprehensive study is essential to assess the recent changes in air pollutants in different regions throughout China. Based on ground-based observations in 367 cities, this study quantitatively analyses the spatio-temporal variation characteristic of urban air pollutants in China from 2014 to 2018.

2. Data and methods

2.1. Study region

This study focuses on the air pollution characteristics over mainland China, which is further classified into seven regions, mainly on the basis of the national administrative participation system. The seven regions are Northeast China, North China, Northwest China, East China, Central China, Southwest China, and South China. Fig. 1 illustrates the division in detail, and Table S1 lists the provinces in each region.

2.2. Data sources

This study used air quality observation data over different regions in mainland China from 13th May 2014 to 31st December 2018. As early as in January 2013, the Ministry of Environmental Protection of China (MEPC) began to release real-time air pollution monitoring information over 74 major cities to the public, including the 6 main components of $PM_{2.5}$, PM_{10}, O_3, SO_2, NO_2 and CO (http://datacenter.mep.gov.cn/). This study employs the urban air quality monitoring data issued by the China Ministry of Ecology and Environment on the website http://beijingair.sinaapp.com/, which has been publishing countrywide air quality data since 13th May 2014. The number of ground-based stations increased from 190 in 2014 to 367 in 2015. We also checked the

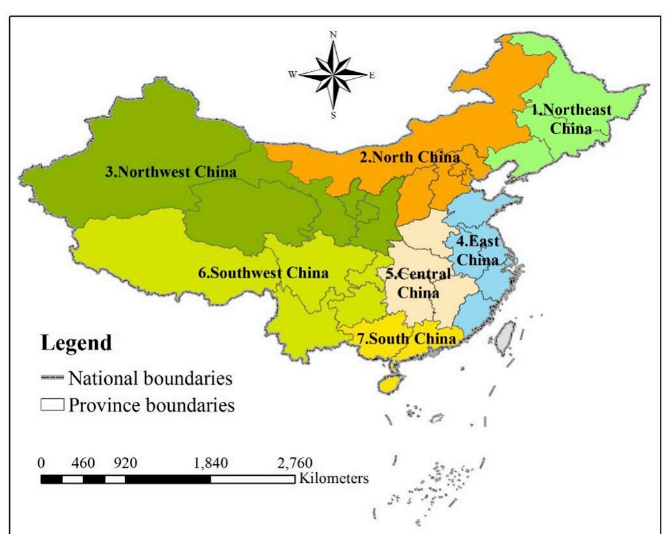

Fig. 1. The classification of seven geographical regions in China.

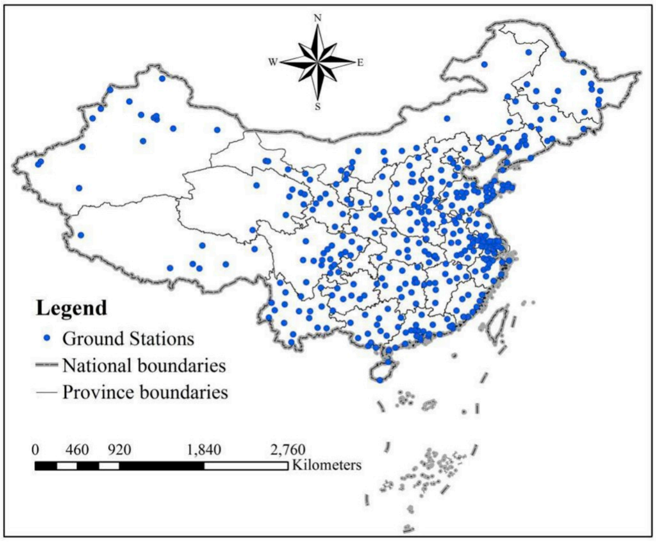

Fig. 2. The distribution of air monitoring stations (367) in mainland China.

potential uncertainties associated with the site differences from 2014 to 2018. By comparing the statistical properties for all pollutant variables obtained using observations at 190 sites and that obtained using observations at all sites from 2014 to 2018, we found that the mean, median and standard deviation of the two groups of data did not differ significantly. Particularly, both data sets show almost the same yearly variation for all variables considered. In order to analyse the temporal and spatial distribution characteristics of air pollutant concentration more comprehensively, all ground-based observation data were used in this study. Fig. 2 shows the spatial distribution of ground observation stations. Actually, the data released by the website have already been adopted by a few previous studies (R. Li et al., 2019; Silver et al., 2018; Zheng et al., 2018). In addition to the ground-based observations data, we also used the emission data of NO_x, SO_2 and smoke from 31 provinces as reported in the China Statistical Yearbook (http://www.stats.gov.cn/tjsj/ndsj/) to study the influence of the emission sources on the air quality.

2.3. Data analysis method

Data quality control (QC) is strictly implemented in this study, which is mainly based on the requirements stated in GB3095-2012 (http://113.108.142.147:20035/emcpublish/) for the validity of air contaminant concentration values and several previous studies (R. Li et al., 2019; Silver et al., 2018). The QC criteria used in this study are as follows. First, hourly values indicated as missing or ≤ 0 are set as invalid. Second, daily average values in a day when there are more than 4 invalid hourly data are set as invalid at every ground station. Third, monthly average values in a month when there are more than 4 invalid daily data are set as invalid at every ground station. Fourth, annual average values when there are more than 324 daily valid data in a year are set as valid and used at every ground station. Fifth, a variability analysis method has been adopted to identify and remove the abnormal hourly observation data.

Here, we briefly describe the variability analysis method, and more details can be found in Shi et al. (2018). The variability analysis method first defines a time window width ΔT. For any observation (A) of the air pollution component at time t over a ground station, we calculate the average (B) over the time window [t-ΔT/2, t+ΔT/2]. If A> 3B or A < B/3, observation A is set as an abnormal value and removed. In this study, the time window width is set as 6 h. Approximately 2% of the data were removed as a result of the quality control by variability analysis.

To analyse the average time duration and proportion of polluted events, we also need to classify the pollution events. The pollution event is defined based on the daily average air quality index (AQI) and $PM_{2.5}$ mass concentration in this study. As well known, AQI is an important comprehensive indicator of air pollution, which is generally used to represent the whole air quality condition. To calculate AQI, it is necessary to obtain the respective AQI values by monitoring the average concentrations of $PM_{2.5}$, PM_{10}, CO, SO_2, NO_2 and O_3 over a certain period of time, and their maximum value is defined as the AQI. More details and standards of AQI calculations can be found in the official documents (http://bz.mee.gov.cn/bzwb/jcffbz/201203/t20120302_224166.shtml). For a given study region or city, when the daily AQI exceeds 100 or the daily $PM_{2.5}$ exceeds 75 $\mu g\, m^{-3}$, the day is recorded as a polluted day that belongs to a polluted event. A polluted event generally begins once the daily AQI exceeds 100 and ends when it falls below 100, or it begins once the daily $PM_{2.5}$ mass concentration exceeds 75 $\mu g\, m^{-3}$ and ends when it falls below 75 $\mu g\, m^{-3}$. However, if there are two pollution events with an interval no longer than 2 days during which the AQI is no less than 95 or the $PM_{2.5}$ concentration is no less than 71.25 $\mu g\, m^{-3}$, they will be recorded as one pollution event. Based on the above definition, we should note that any pollution event defined here shall last at least one day.

In this study, the time average of air pollution components was analyzed, including daily, monthly, seasonal, and yearly averages. It should be noted that in this study, the ozone calculation uses the maximum daily 8-h average ozone concentration (O_3MDA8). The spring, summer, autumn and winter are defined as March to May, June to August, September to November, and December to February of the following year, respectively. Moreover, in order to clarify the average distribution pattern and probability of occurrence of different air pollutants, we also analyzed the probability distribution function (PDF) in this study. The specific formula is as follows.

$$P(a \leq x \leq b) = \int_a^b f_X(x)dx$$

where $P(a \leq x \leq b)$ is the probability of occurrence for air pollutant X with values between a and b, and $f_X(x)$ is frequency of occurrence of air pollutant at a specific value of x between a and b. Note that the air pollutant X can be $PM_{2.5}$, PM_{10}, SO_2, NO_2, O_3MDA8, CO and AQI.

3. Results and discussion

3.1. Spatial and temporal distribution of the air quality index in China

Fig. 3 shows the temporal variation and statistical characteristics of the AQI averaged in mainland China. The AQI shows clear seasonal variations, with high values in winter and low values in summer. In both summer and winter, there are clear decreasing trends in the AQI from 2014 to 2018. The annually averaged values of the AQI are 82.68 and 69.49 in 2014 and 2018, respectively. Moreover, the median values of the AQI in 2014 and 2018 are 78.04 and 65.37, respectively. It is clear that there is a significant decreasing trend in the air quality from 2014 to 2018. Considering the large range of the AQI values in each year and the existence of high AQI values, heavy pollution episodes represented by extreme AQI values still exist in each year.

Considering that AQI is from the maximum value of six individual pollutants, we should note that certain uncertainties could be introduced by using AQI to indicate the relative pollution status while it is widely used by the government in China. Fig. 4 further shows the spatial distribution of the seasonally averaged AQI in spring, summer, autumn, and winter during the study period from 2014 to 2018. The spatial distributions of seasonally averaged AQI are similar to each other in the four seasons, with AQI being the highest in winter and lowest in summer, consistent with the results in Fig. 3. While this is generally explained as the higher air quality in summer than in winter, we should note that the AQI values are more likely representative of $PM_{2.5}$ in

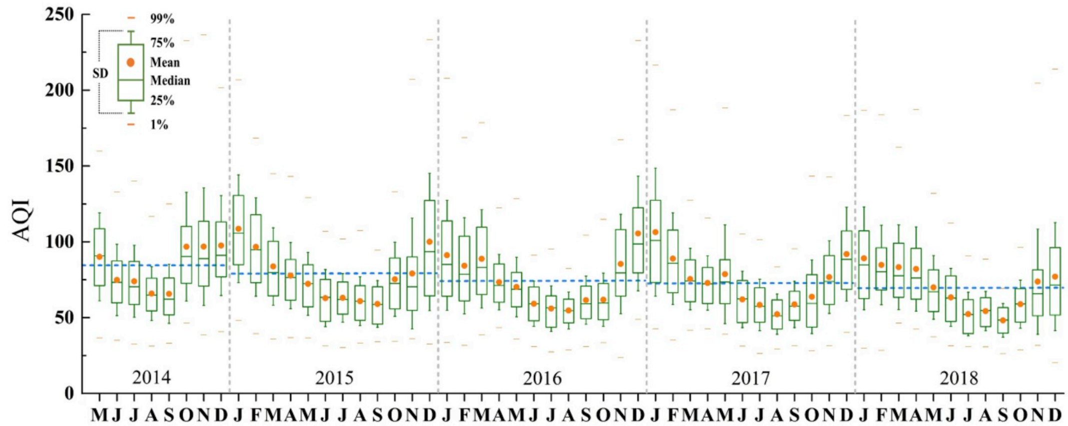

Fig. 3. Temporal variation of statistical characteristics of the AQI. SD indicates the standard deviation, 1%, 25%, 75% and 99% indicate the percentages of samples from low to high in order.

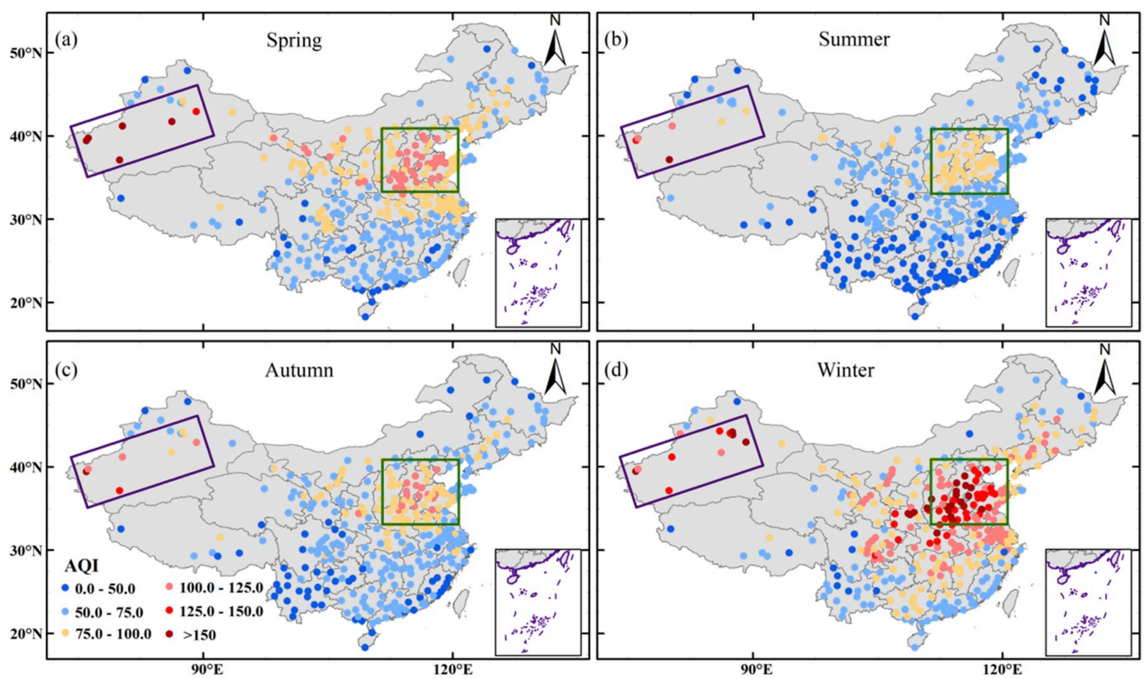

Fig. 4. The spatial distribution of the seasonally averaged AQI: (a) spring for months from March to May, (b) summer for months from June to August, (c) autumn for months from September to November, and (d) winter for months from December to February of the following year.

winter and O_3 in summer. There are two regions with serious air pollution in all four seasons: cities in the North China Plain area (circled by a block green line) and cities in the central and western Xinjiang area (circled by a block purple line). The Beijing-Tianjin-Hebei region is the largest economic region in the North China Plain area, with about 9.0% of national coal consumption and more than 20% of national steel production in 2013 (NBS, 2014). Correspondingly, $PM_{2.5}$ has been the most significant contributing air pollutant in this region (Li et al., 2018; Shao et al., 2018). Particularly, the combustion of fossil fuels for heating systems in winter increases winter pollution in North China (Y.J. Li et al., 2017; Luo et al., 2017; Shen et al., 2019). On the other hand, the North China region encounters the least rainfall and convective activities in winter. Both fossil fuel burning and weak convection make the number of polluted cities the largest in winter compared with the other seasons (Tian et al., 2019; Yan et al., 2018). Cities in the central and western areas of Xinjiang are located around the Taklimakan Desert and its adjacent drylands, and the transport of dust aerosols make the PM_{10} mass concentration relatively high (Chen et al., 2017a; Ji et al., 2018; Yuan et al., 2019). The high PM_{10} is likely the reason for the high AQI values in the central and western areas of Xinjiang in all four seasons (Chen et al., 2017a,b). In spring, more dust is raised by strong winds from more exposed land surfaces, and it moves along a certain route: Taklimakan Desert - Hexi Corridor - Loess Plateau - North China Plain, making the area along this transmission route become an obvious highly polluted area, as shown in Fig. 4a (Chen and Wang, 2015; Chen et al., 2017a).

In contrast to the two seriously polluted regions, the AQI values in the Yunnan-Guizhou Plateau and cities in Southeast China are only about 1/3 that in other two regions in all four seasons, indicating much better air quality. This is mainly due to the relatively remote nature of the Yunnan-Guizhou Plateau, which has a relatively clean atmospheric environment compared to the atmospheric pollution caused by large-scale urbanization and industrialization in central and eastern China. In addition, previous studies have found that there are strong and frequent precipitation in southern and eastern parts of the Yunnan–Guizhou Plateau (Q.P. Cheng et al., 2019; Shi et al., 2015), which

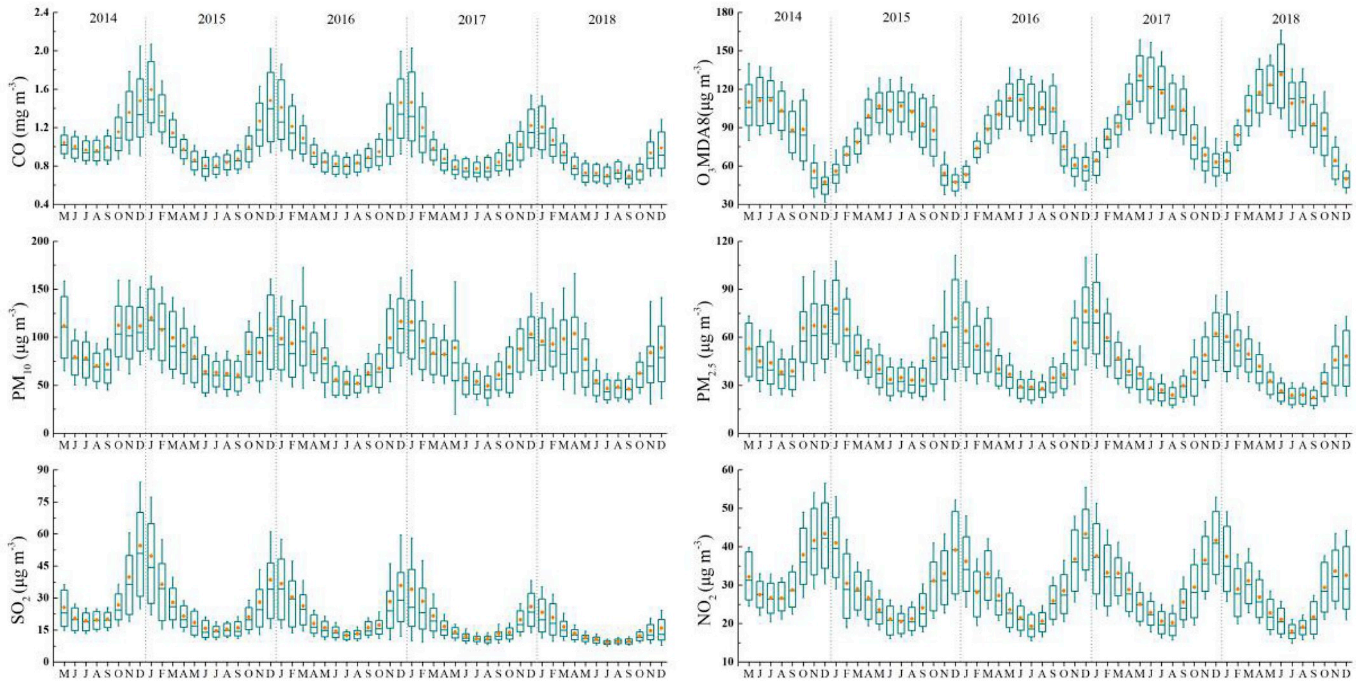

Fig. 5. The temporal variation of six conventional pollution indicators (including CO, NO_2, O_3MDA8, PM_{10}, $PM_{2.5}$ and SO_2), the meanings of the symbols are the same as that shown in Fig. 3.

could scavenge the aerosol pollutants and make the air quality in this region high. Furthermore, air control measures taken by the government have helped maintain relatively good air quality in the region without considering the change of meteorological conditions.

3.2. Trends of six types of air pollution components in China

We also investigated the temporal trends of air pollutants other than the AQI, including $PM_{2.5}$, PM_{10}, SO_2, NO_2, CO, and O_3MDA8, which are shown in Fig. 5. Similar to the AQI shown in Fig. 4, there is an obvious

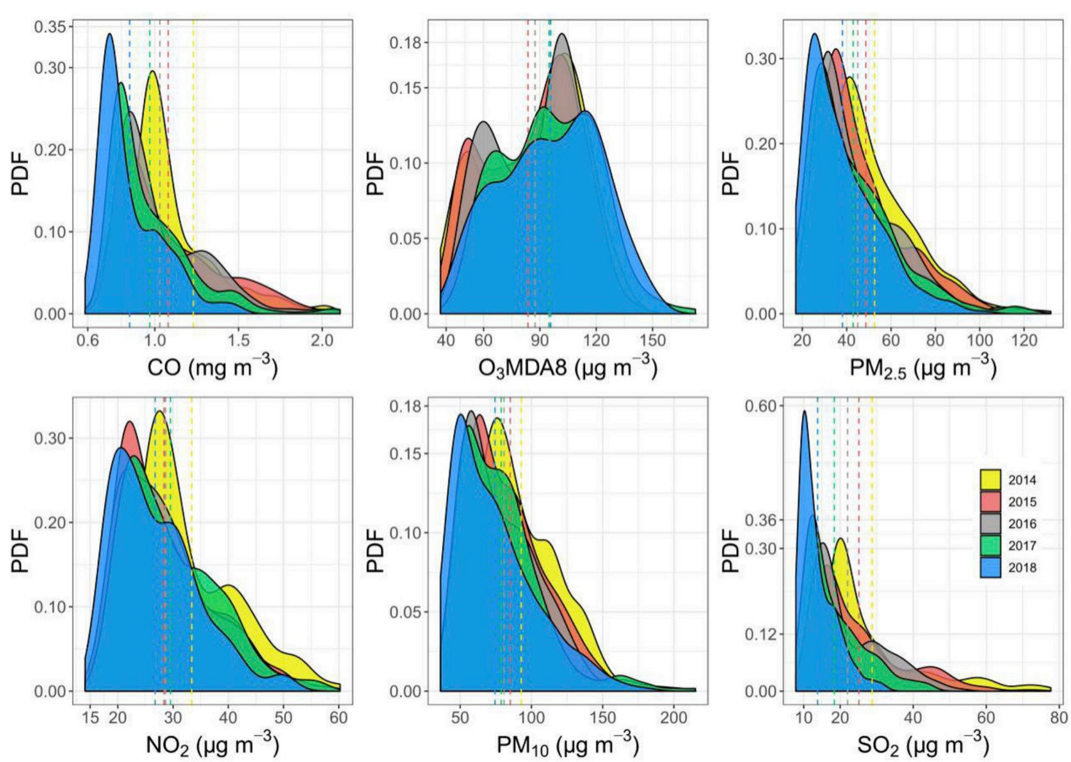

Fig. 6. The probability distribution function (PDF) of daily averages of CO, NO_2, O_3MDA8, PM_{10}, $PM_{2.5}$ and SO_2 in 2014, 2015, 2016, 2017, and 2018. The dashed lines indicate the means of the air pollutant in the corresponding year. The colours represent the years. (For interpretation of the references to colour in this figure legend, the reader is referred to the Web version of this article.)

annual periodicity or seasonal cycle. Air pollutants other than O_3MDA8, which are found in Fig. 5, demonstrate the same seasonal variations as the AQI, with high values in winter and low values in summer. Similar to the AQI, $PM_{2.5}$, PM_{10}, SO_2, NO_2, and CO show clear decreasing trends in both summer and winter from 2014 to 2018. For O_3MDA8, because of strong solar radiation and high temperature in summer, atmospheric photochemical reactions of airborne oxynitrides and volatile organic compounds (VOCs) are so active that much more ozone is produced, making the O_3MDA8 concentration high in summer and low in winter (Bai et al., 2018; K. Li et al., 2019). Unlike other pollutants, O_3MDA8 shows an increasing trend in both summer and winter from 2014 to 2018. One reason is that air pollution control measures reduce the air particles or aerosols more significantly than the NO_2 and VOCs, allowing more solar radiation to reach the low atmosphere and resulting in more significant photochemical reactions, which generate more ozone (Fang et al., 2018; K. Li et al., 2019).

Fig. 6 shows the probability distribution function of CO, NO_2, O_3MDA8, PM_{10}, $PM_{2.5}$ and SO_2 in 2014, 2015, 2016, 2017, and 2018. During the last 5 years, CO, $PM_{2.5}$, PM_{10} and SO_2 have continuously decreased. In contrast, NO_2 decreased significantly during 2014–2015 and 2017–2018 but increased by 3.5% from 2015 to 2017. Compared with the 2014 data, the average CO, $PM_{2.5}$, PM_{10}, NO_2 and SO_2 decreased by 25%, 28%, 20%, 20% and 52%, respectively, in 2018. The PDFs of CO, $PM_{2.5}$, PM_{10}, SO_2 and NO_2 roughly show single mode distributions, with the maximum occurrence frequency at relatively low values of these air pollutants. China's countrywide air quality control policies have contributed much to the abatement (J. Cheng et al., 2019; Y. Liu et al., 2019). There were even more rigid industrial emission limits and air quality control measures during several large national activities, e.g., the Asia-Pacific Economic Cooperation (APEC) conference in 2014 and the China Victory Day Parade in 2015 (Ren et al., 2019; Sun et al., 2016). Many studies have indicated that industrial emissions are the main reason for China's pollution problems (Krotkov et al., 2016; Liang et al., 2017; Zhao et al., 2019). Fig. 6 also shows an increasing trend in O_3 in China from 2014 to 2018, which has already elicited concerns from around the world (K. Li et al., 2019). Compared with that in 2015, O_3MDA8 increased by 4.5%, 13% and 14% in the following three years. Unlike the PDFs of the other air pollutants, the PDF of O_3MDA8 demonstrates a bimodal distribution, with a peak occurrence at a relatively low value of 50–60 $\mu g\ m^{-3}$ and a high value of 105–115 $\mu g\ m^{-3}$. These findings can help us understand the variation features of different types of air pollutants in China.

Fig. 7 shows the relative change in CO, NO_2, O_3MDA8, PM_{10}, $PM_{2.5}$ and SO_2 across mainland China in 2018 compared to the 2014 data. Relative to the 2014 data, 87%, 63%, 78%, 89% and 93% of stations around the country monitored a decline in CO, NO_2, PM_{10}, $PM_{2.5}$ and SO_2 in 2018, respectively. According to Figs. 6 and 7, among the 6 types of air pollutants, the reduction of SO_2 is the most substantial, followed

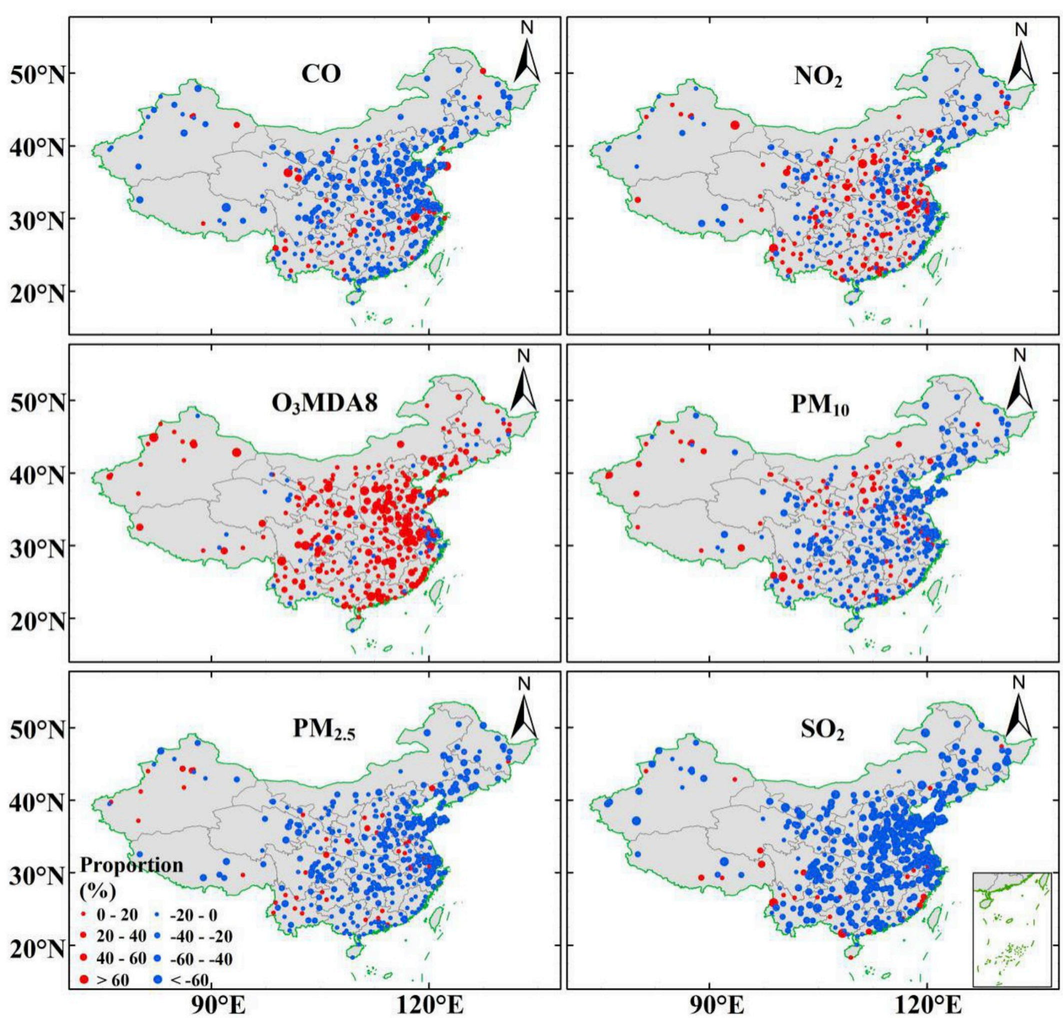

Fig. 7. Relative change in CO, NO_2, O_3MDA8, PM_{10}, $PM_{2.5}$ and SO_2 across mainland China during 2018 compared to that in 2014. Blue and red in the figure indicate the positive and negative changes, respectively. The size of the sites in the figure reflects the proportion magnitude of the increasing or decreasing amount. (For interpretation of the references to colour in this figure legend, the reader is referred to the Web version of this article.)

by $PM_{2.5}$ and CO. The largest decrease in SO_2 occurred for cities located in the North China Plain area and the Yangtze River Economic Belt. Considering that there are still a large number of stations with increasing trends in NO_2, the control of NO_2 emissions could be the emphasis of next steps in air pollution control. Unlike other air pollutants, O_3MDA8 continued to increase during the study period for approximately 83% of city monitoring stations. Therefore, ozone will become another focus of air pollution control in the future.

All these analyses suggest that the mass concentration of CO, NO_2, PM_{10}, $PM_{2.5}$ and SO_2 decreases while the mass concentration of ozone continues to increase. Therefore, the conclusion that China's air quality is improving year by year does not include all air pollution components. Moreover, although China's air quality is improving, the seasonality of heavy pollution is still very obvious. Specifically, the mean and high values of SO_2, $PM_{2.5}$, and CO decreased in each month, especially in autumn and winter, however, there was no significant decrease in the high concentration values of PM_{10} and NO_2 during the heavy pollution season. The O_3MDA8 increased rapidly during the summer and the average concentration has exceeded 120 $\mu g\ m^{-3}$. These findings help us recognize the temporal variation of air pollutants, along with the information of key pollutants in each season.

3.3. Spatial differences of air pollutant change

Fig. 7 shows that the relative changes in these air pollution components have clear and different spatial variations. The average relative changes in CO, NO_2, O_3MDA8, PM_{10}, $PM_{2.5}$ and SO_2 are −17%, −3%, 20%, −11%, −20% and −39%, respectively. For most stations, there are significant decreases in CO, SO_2, PM_{10} and $PM_{2.5}$. In contrast, a roughly similar number of stations show increasing and decreasing NO_2, and there are more stations with significantly increasing O_3MDA8. These results imply that there are significant reductions in the emissions of SO_x but not as much of a reduction in the emission of NO_x. With a decreasing number of air particles, increasing solar radiation increases the generation of ozone, which is dependent on ultraviolet radiation, VOCs and NO_2.

Fig. 8 compares the averaged air pollutants in the seven geographical regions classified in Fig. 2 for 2014–2018. The minimum and average values of the air pollutants vary little among the seven regions; however, the maximum values of the air pollutants vary greatly among the regions. In other words, extreme pollution events could vary more with regions than weak pollution events. Previous studies indicate that differences in the underlying surface, meteorological conditions, and air pollutant emissions among the regions strengthen the differences in the maximum values of air pollutants (Chen et al., 2018; Ding et al., 2017; Guan et al., 2019; Shao et al., 2018). Fig. 8 suggests that there are low values of all types of air pollutants in South China, high CO in North China and Northwest China, high NO_2 in North China and East China, high PM_{10} in Northwest China, high $PM_{2.5}$ in North China and Central China, and high SO_2 in North China and Northeast China.

Fig. 9 further shows the anomalies of seven air pollutant variables (AQI, CO, NO_2, SO_2, $PM_{2.5}$, PM_{10}, and O_3) in the seven geographical regions in China for the period from 2014 to 2018. Despite the fluctuations, the findings are similar to those shown earlier: there are clear decreasing trends for CO, NO_2, SO_2, and $PM_{2.5}$ in all 7 regions, while O_3MDA8 demonstrates a clear increasing trend for 2014–2018. For all 7 regions, the air pollutant component with the largest reduction is SO_2, with reduction rates greater than 50%. The rapid reduction of SO_2 most likely benefits from the application of fuel desulphurization technology and similar techniques in industries (R. Li et al., 2019; Liu et al., 2018). Fig. 9 also shows clear decreasing trends for PM_{10} in all regions except Northwest China, where the dust aerosols make PM_{10} difficult to reduce. It should be noted that analyses only focusing on individual contaminants (e.g., $PM_{2.5}$, SO_2) are not enough for air quality assessment, particularly considering the increase in ozone during recent years. We can evaluate the air quality based on the AQI values, which show clear decreasing trends in all regions except Northwest China. In Northwest China, there have been no clear trends in the AQI over the last several

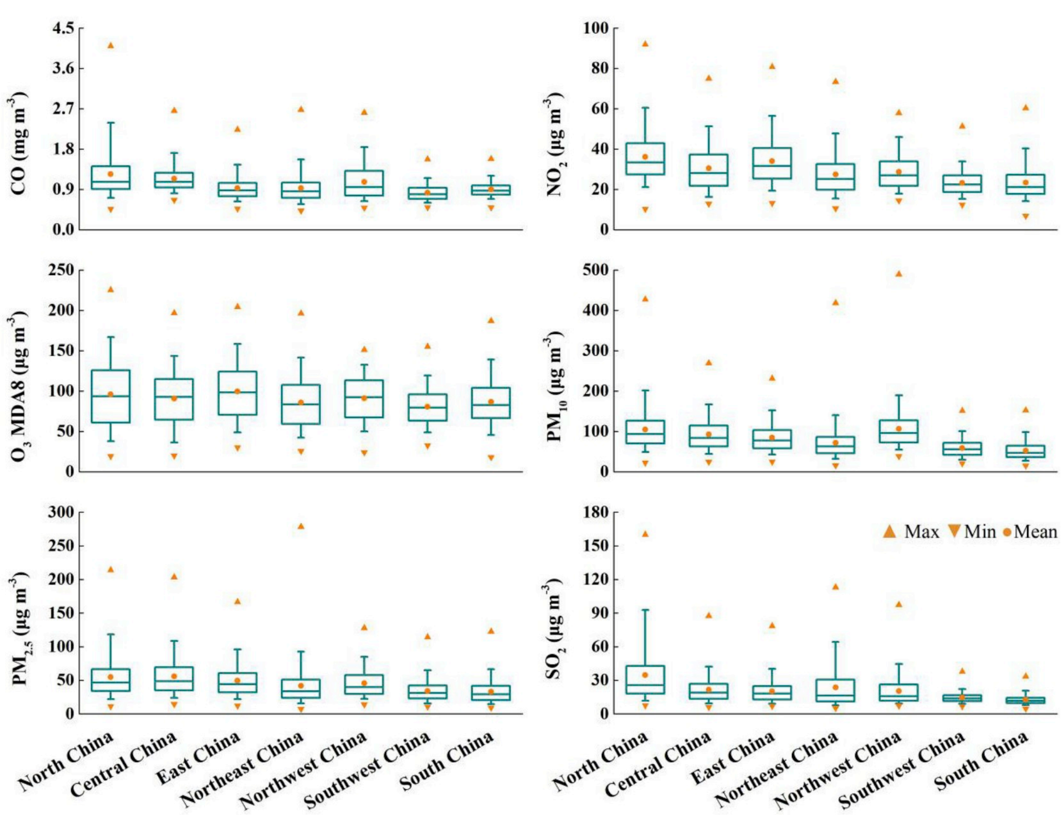

Fig. 8. The comparison of averaged air pollutants in the seven geographical regions classified in Fig. 2 for 2014–2018.

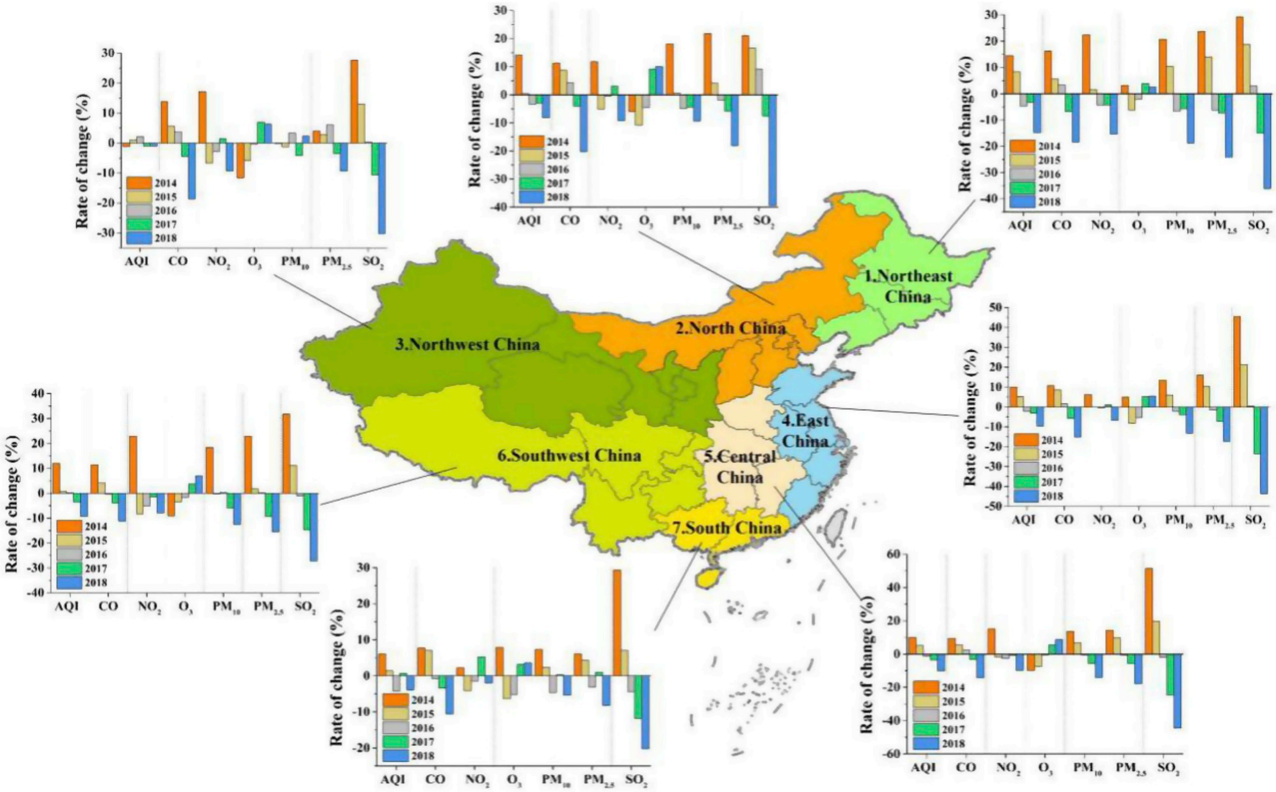

Fig. 9. The anomalies of seven variables that represent air pollutants in the seven geographical regions in China from 2014 to 2018.

Table 1
Duration (day) and proportion (%) of pollution weather events in 2014–2018 for the seven regions based on two definitions: one is based on the AQI and the other is based on $PM_{2.5}$. Note that NE, N, NW, E, C, SW and S represent Northeast, North, Northwest, East, Central, Southwest, and South China region, respectively; D (day) and P (%) refer to Duration and Proportion, respectively.

		1. NE		2. N		3. NW		4. E		5. C		6. SW		7. S	
		D	P	D	P	D	P	D	P	D	P	D	P	D	P
AQI	2014	3	27	4	50	4	27	3	34	5	43	3	10	2	6
	2015	3	21	4	40	6	36	4	25	7	33	5	8	5	7
	2016	2	11	3	31	7	34	3	22	6	30	3	2	2	2
	2017	3	16	3	28	6	25	3	16	4	22	7	6	3	5
	2018	2	9	3	29	6	32	3	15	4	20	2	1	4	4
$PM_{2.5}$	2014	3	23	3	36	2	10	2	20	5	33	3	6	2	3
	2015	3	16	3	23	3	11	3	18	7	27	3	4	5	5
	2016	2	7	3	22	4	17	3	14	7	25	1	0	1	0
	2017	3	12	3	15	3	12	3	12	4	19	4	3	3	4
	2018	2	3	2	11	2	5	3	8	4	13	2	1	3	3

D (day) and P (%) refer to Duration and Proportion, respectively.

years.

Air pollution events can be assessed for their occurrence frequency and duration time in every case. Table 1 shows the duration (days) and proportion (%) of the pollution weather events for 7 regions in 2014–2018 based on the definitions of AQI and $PM_{2.5}$. For most regions, both the proportion and duration of pollution events decreased during the study period of 2014–2018. The average decreasing rates of occurrence frequency of air pollution events that are defined based on the AQI ($PM_{2.5}$) are 17% $year^{-1}$ (22% $year^{-1}$), 10% $year^{-1}$ (17% $year^{-1}$), 14% $year^{-1}$ (15% $year^{-1}$), 14% $year^{-1}$ (15% $year^{-1}$), and 22% $year^{-1}$ (22% $year^{-1}$) for Northeast China, North China, East China, Central China, and Southwest China, respectively. Moreover, the decreasing rates of time duration of air pollution events that are defined based on the AQI ($PM_{2.5}$) are 6% $year^{-1}$ (9% $year^{-1}$), 2% $year^{-1}$ (9% $year^{-1}$), 7% $year^{-1}$ (2% $year^{-1}$), and 8% $year^{-1}$ (11% $year^{-1}$) for Northeast China, North China, Central China, and Southwest China, respectively. For the pollution events classified using $PM_{2.5}$, only North China and Central China had more than 10% pollution event days in all study years. In contrast, for the pollution events classified using the AQI, in addition to North China and Central China, Northwest China also had a large proportion (32%) of pollution event days in all study years. The differences in pollution events in Northwest China based on the AQI and $PM_{2.5}$ are associated with the impact of dust aerosols. Dust aerosols in Northwest China are heavy and change little with time for the study period (Chen et al., 2017b; Yuan et al., 2019), so they contribute greatly to PM_{10}, making the AQI high and contributing little to the $PM_{2.5}$.

Air pollutants are from both natural and anthropogenic emissions, including desert dust, biomass combustion, and fossil fuel combustion, among which emissions caused by industrial activities are the main cause of air pollution in many areas (Chen et al., 2018; Zhao et al., 2019;

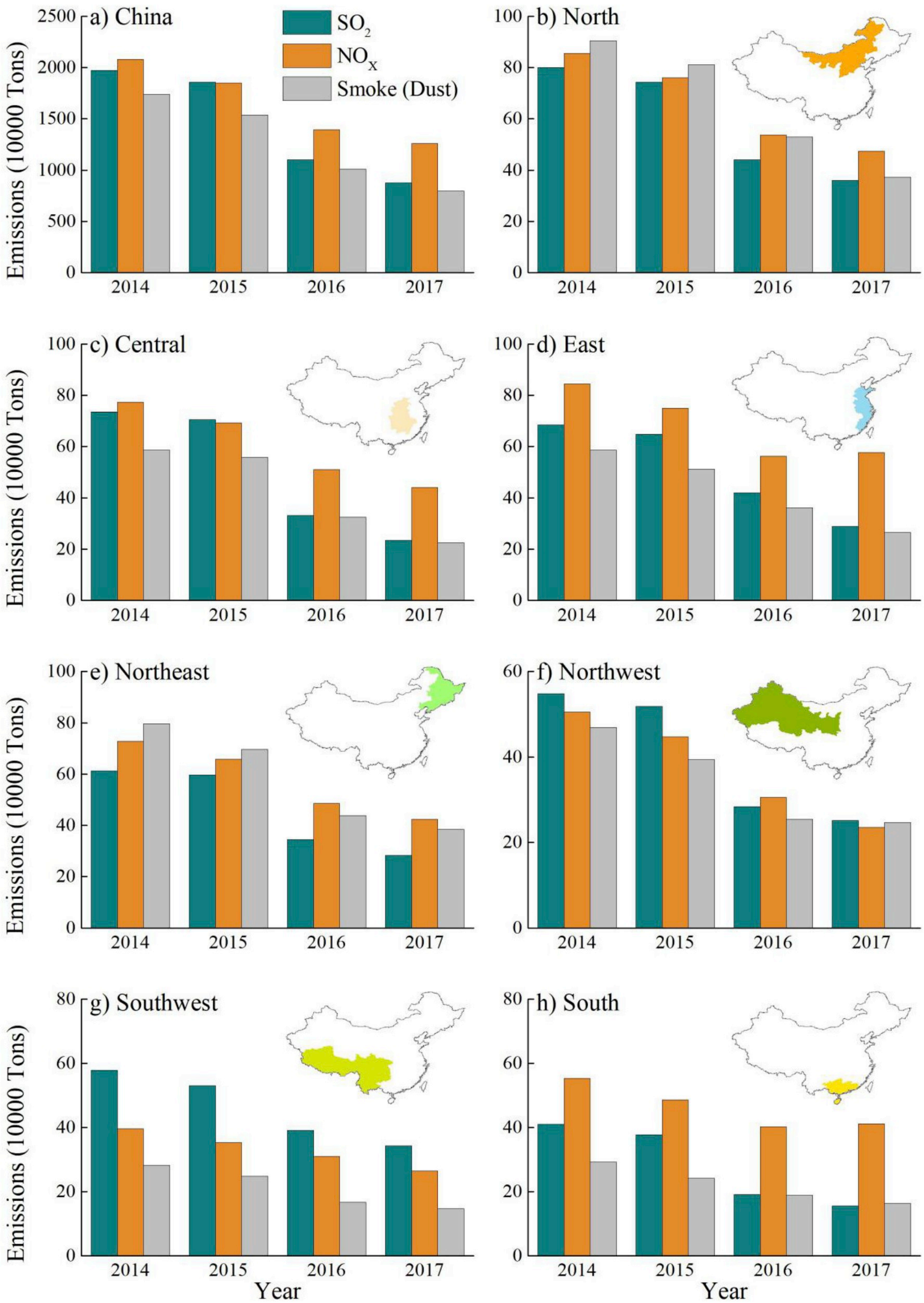

Fig. 10. Annual emissions of different kinds of exhaust gases from 2014 to 2017 in China along with the seven regions within.

Zheng et al., 2018; Zhou and Zhou, 2017). Meteorological conditions and precursor gases also have comprehensive impacts on the transport of air pollutants and the generation of secondary aerosols (Chen and Wang, 2015; Zhao et al., 2019). Considering that the meteorological conditions in China have contributed relatively little to the improvement of air quality in recent years and have not changed significantly during recent years (Chen and Wang, 2015; J. Cheng et al., 2019; Pei and Yan, 2018; Xu et al., 2018; Zhang et al., 2016), the air quality improvements found in this study should be mainly caused by rigid air quality control policies and emission reduction measures.

Fig. 10 shows the regional emissions (industrial and life) of SO_2, NO_x, and smoke (dust) in China during 2014–2017. The emissions of SO_2, NO_x and the sum of smoke and dust have been reduced in all regions of China by 3,663,400, 2,730,600 and 3,148,300 tons, respectively. This supports the decreasing trends in air pollutants found earlier. For each region in China, we can also see clear decreasing trends in the regional emissions of SO_2, NO_x, and smoke (dust). Unfortunately, this study has not quantified the influences of the above-mentioned factors on air quality in different seasons because the available emission data we obtained are year based.

As indicated above, the improvement of air quality is highly associated with the air pollution control act in China. The governments of states and provinces have continued to carry out industry clean production audits, desulphurization, denitrification, dust removal renovation projects and upgrading of pollution facilities in key industries (Ebenstein et al., 2017; Ma et al., 2017). Actually, satellite-based remote sensing studies have found similar results about the change of air pollution during recent years due to the strict emission control act. For example, the SO_2 decreased about 50% based on satellite measurements from January 2014 to July 2016 (Karplus et al., 2018), and in the North China Plain even dropped by more than 50% between 2005 and 2015 (Krotkov et al., 2016). In northern China, Zheng et al. (2018) found that NO_2 and SO_2 declined at an average annual rate of 8.1% and 1.6% from 2011 to 2016 respectively using OMI satellite data. The researchers also found that $PM_{2.5}$ concentrations showed a downward trend in 2007–2013 (Ma et al., 2015) and 2006–2015 (Lin et al., 2018), respectively.

The temporal variation of air pollution should be associated with the changes of both meteorological conditions and aerosol emissions. As indicated by X.Y. Zhang et al. (2019), the meteorological conditions worsened in 2014 and 2015 and improved in 2016 and 2017 relative to those in 2013 in most of our study regions. They also indicated that the emission reduction measures are the major contributing factor for the $PM_{2.5}$ reduction from 2013 to 2017 in the Beijing-Tianjin-Hebei region. Furthermore, Xu et al. (2018) showed that 13.6% changes of the national average $PM_{2.5}$ mass concentration were caused by changes in meteorological conditions between January 2017 and January 2016. In addition, J. Cheng et al. (2019) indicated that the contributions of changes in meteorological conditions, reductions in local emissions, and reductions in regional emissions to Beijing's air quality improvement are 12.1%, 65.4%, and 22.5%, respectively from 2013 to 2017. Combined with these findings from previous studies, the air quality improvements found in this study should be mainly caused by rigid air quality control policies and emission reduction measures.

4. Conclusions

Based on the national air quality ground observation database, with data from more than 300 cities from May 2014 to December 2018, this study provides a comprehensive analysis of the spatial-temporal distribution characteristics of air pollution over the 7 classified regions in China. Although some studies have analyzed $PM_{2.5}$, O_3 and other air pollution indicators in key cities and China, this study still provides valuable information about the changes in the concentrations of various pollutants in China over the past five years.

In terms of time change, the AQI, CO, NO_2, SO_2, PM_{10} and $PM_{2.5}$ decreased by 16%, 25%, 20%, 52%, 20% and 28%, respectively, in 2018 compared to 2014. In contrast, O_3MDA8 continuously increased at an average rate of 4.6% per year for the study period. Furthermore, compared to the 2014 data, 87%, 63%, 78%, 89% and 93% of stations around the country monitored declines of CO, NO_2, PM_{10}, $PM_{2.5}$ and SO_2 in 2018, respectively.

The air pollution components demonstrate distinct differences in spatial distribution, with high values of CO in North China and Northwest China, NO_2 in North China and East China, PM_{10} in Northwest China, $PM_{2.5}$ in North China and Central China, and SO_2 in North China and Northeast China. The time duration of air pollution events have decreased during recent years, which are 6% $year^{-1}$, 2% $year^{-1}$, 7% $year^{-1}$, and 8% $year^{-1}$ based on AQI values, and 9% $year^{-1}$, 9% $year^{-1}$, 2% $year^{-1}$ and 11% $year^{-1}$ based on $PM_{2.5}$ values, for Northeast China, North China, Central China and Southwest China, respectively. In the past five years, Northeast China, Central China and North China were the three regions with the largest decline in the AQI. Roughly, air pollution was most serious in the North China Plain and in cities in central and western Xinjiang Province.

Overall, the constant improvement of air quality are likely associated with rigorous emission control acts in China. From 2014 to 2017, the emissions of SO_2, NO_x and the sum of smoke and dust were reduced in all regions of China by 3,663,400, 2,730,600 and 3,148,300 tons, respectively. The statistical results of the 7 regions also conform to the decreasing trends. However, there is also a trend of increasing O_3 and slowly decreasing NO_2. In future, we should continue to optimize our energy structure of cities to reduce potential emissions of pollutants, for example, by reducing the use of fossil fuel and promoting the development of clean energy. In addition, urban air quality can be improved through reasonable urban planning and layout.

Declaration of competing interest

The authors declare that they have no known competing financial interests or personal relationships that could have appeared to influence the work reported in this paper.

Acknowledgements

This work was supported by the Beijing Municipal Commission of science and technology (grant D171100007917001), the National Natural Science Foundation of China (grants 91837204, 41575143), the State Key Laboratory of Earth Surface Processes and Resource Ecology (2017-ZY-02), and the Fundamental Research Funds for the Central Universities (2017EYT18, 312231103). The air quality data are downloaded from the public website of the China Ministry of Ecology and Environment (http://beijingair.sinaapp.com/), and the emission data are obtained from the China Statistical Yearbook (http://www.stats.gov.cn/tjsj/ndsj/).

Appendix A. Supplementary data

Supplementary data to this article can be found online at https://doi.org/10.1016/j.atmosenv.2019.117066.

References

Bai, J.H., de Leeuw, G., van der A, R., De Smedt, I., Theys, N., Van Roozendael, M., Sogacheva, L., Chai, W.H., 2018. Variations and photochemical transformations of atmospheric constituents in North China. Atmos. Environ. 189, 213–226. https://doi.org/10.1016/j.atmosenv.2018.07.004.

Brauer, M., Freedman, G., Frostad, J., van Donkelaar, A., Martin, R.V., Dentener, F., van Dingenen, R., Estep, K., Amini, H., Apte, J.S., Balakrishnan, K., Barregard, L., Broday, D., Feigin, V., Ghosh, S., Hopke, P.K., Knibbs, L.D., Kokubo, Y., Liu, Y., Ma, S., Morawska, L., Sangrador, J.L., Shaddick, G., Anderson, H.R., Vos, T., Forouzanfar, M.H., Burnett, R.T., Cohen, A., 2016. Ambient air pollution exposure estimation for the global burden of disease 2013. Environ. Sci. Technol. 50 (1), 79–88. https://doi.org/10.1021/acs.est.5b03709.

Chen, H.P., Wang, H.J., 2015. Haze Days in North China and the associated atmospheric circulations based on daily visibility data from 1960 to 2012. J. Geophys. Res.: Atmosphere 120 (12), 5895–5909. https://doi.org/10.1002/2015jd023225.

Chen, J., Zhou, C.S., Wang, S.J., Hu, J.C., 2018. Identifying the socioeconomic determinants of population exposure to particulate matter ($PM_{2.5}$) in China using geographically weighted regression modeling. Environ. Pollut. 241, 494–503. https://doi.org/10.1016/j.envpol.2018.05.083.

Chen, S.Y., Huang, J.P., Kang, L.T., Wang, H., Ma, X.J., He, Y.L., Yuan, T.G., Yang, B., Huang, Z.W., Zhang, G.L., 2017. Emission, transport, and radiative effects of mineral dust from the Taklimakan and Gobi deserts: comparison of measurements and model results. Atmos. Chem. Phys. 17 (3), 2401–2421. https://doi.org/10.5194/acp-17-2401-2017.

Chen, S.Y., Huang, J.P., Qian, Y., Zhao, C., Kang, L.T., Yang, B., Wang, Y., Liu, Y.Z., Yuan, T.G., Wang, T.H., Ma, X.J., Zhang, G.L., 2017. An overview of mineral dust modeling over East Asia. J. Meteorol. Res. 31 (4), 633–653. https://doi.org/10.1007/s13351-017-6142-2.

Cheng, J., Su, J.P., Cui, T., Li, X., Dong, X., Sun, F., Yang, Y.Y., Tong, D., Zheng, Y.X., Li, Y.S., Li, J.X., Zhang, Q., He, K.B., 2019. Dominant role of emission reduction in $PM_{2.5}$ air quality improvement in Beijing during 2013–2017: a model-based decomposition analysis. Atmos. Chem. Phys. 19 (9), 6125–6146. https://doi.org/10.5194/acp-19-6125-2019.

Cheng, Q.P., Gao, L., Zuo, X.A., Zhong, F.L., 2019. Statistical analyses of spatial and temporal variabilities in total, daytime, and nighttime precipitation indices and of extreme dry/wet association with large-scale circulations of Southwest China, 1961–2016. Atmos. Res. 219, 166–182. https://doi.org/10.1016/j.atmosres.2018.12.033.

Cohen, A.J., Brauer, M., Burnett, R., Anderson, H.R., Frostad, J., Estep, K., Balakrishnan, K., Brunekreef, B., Dandona, L., Dandona, R., Feigin, V., Freedman, G., Hubbell, B., Jobling, A., Kan, H.D., Knibbs, L., Liu, Y., Martin, R., Morawska, L., Pope, C.A., Shin, H., Straif, K., Shaddick, G., Thomas, M., van Dingenen, R., van Donkelaar, A., Vos, T., Murray, C.J.L., Forouzanfar, M.H., 2017. Estimates and 25-year trends of the global burden of disease attributable to ambient air pollution: an analysis of data from the Global Burden of Diseases Study 2015. The Lancet 389 (10082), 1907–1918. https://doi.org/10.1016/s0140-6736(17)30505-6.

Ding, J.Y., Miyazaki, K., van der A, R.J., Mijling, B., Kurokawa, J-i., Cho, S., Janssens-Maenhout, G., Zhang, Q., Liu, F., Levelt, P.F., 2017. Intercomparison of NO_x emission inventories over East Asia. Atmos. Chem. Phys. 17 (16), 10125–10141. https://doi.org/10.5194/acp-17-10125-2017.

Ebenstein, A., Fan, M.Y., Greenstone, M., He, G.J., Zhou, M.G., 2017. New evidence on the impact of sustained exposure to air pollution on life expectancy from China's Huai River Policy. Proc. Natl. Acad. Sci. U. S. A 114 (39), 10384–10389. https://doi.org/10.1073/pnas.1616784114.

Fang, X.K., Park, S., Saito, T., Tunnicliffe, R., Ganesan, A.L., Rigby, M., Li, S.L., Yokouchi, Y., Fraser, P.J., Harth, C.M., Krummel, P.B., Mühle, J., O'Doherty, S., Salameh, P.K., Simmonds, P.G., Weiss, R.F., Young, D., Lunt, M.F., Manning, A.J., Gressent, A., Prinn, R.G., 2018. Rapid increase in ozone-depleting chloroform emissions from China. Nat. Geosci. 12 (2), 89–93. https://doi.org/10.1038/s41561-018-0278-2.

Guan, D.B., Su, X., Zhang, Q., Peters, G.P., Liu, Z., Lei, Y., He, K.B., 2014. The socioeconomic drivers of China's primary $PM_{2.5}$ emissions. Environ. Res. Lett. 9 (2), 024010 https://doi.org/10.1088/1748-9326/9/2/024010.

Guan, T.J., Xue, T., Gao, S.H., Hu, M., Liu, X., Qiu, X.H., Liu, X.H., Zhu, T., 2019. Acute and chronic effects of ambient fine particulate matter on preterm births in Beijing, China: a time-series model. Sci. Total Environ. 650, 1671–1677. https://doi.org/10.1016/j.scitotenv.2018.09.279.

Hadley, M.B., Vedanthan, R., Fuster, V., 2018. Air pollution and cardiovascular disease: a window of opportunity. Nat. Rev. Cardiol. 15, 193. https://doi.org/10.1038/nrcardio.2017.207.

Herrera-Estrada, J.E., Diffenbaugh, N.S., Wagner, F., Craft, A., Sheffield, J., 2018. Response of electricity sector air pollution emissions to drought conditions in the western United States. Environ. Res. Lett. 13 (12), 124032. https://doi.org/10.1088/1748-9326/aaf07b.

Ji, G.X., Zhao, J.C., Yang, X., Yue, Y.L., Wang, Z., 2018. Exploring China's 21-year PM_{10} emissions spatiotemporal variations by DMSP-OLS nighttime stable light data. Atmos. Environ. 191, 132–141. https://doi.org/10.1016/j.atmosenv.2018.07.045.

Kang, H.Q., Zhu, B., van der A, R.J., Zhu, C.M., de Leeuw, G., Hou, X.W., Gao, J.H., 2019. Natural and anthropogenic contributions to long-term variations of SO_2, NO_2, CO, and AOD over East China. Atmos. Res. 215, 284–293. https://doi.org/10.1016/j.atmosres.2018.09.012.

Karplus, V.J., Zhang, S., Almond, D., 2018. Quantifying coal power plant responses to tighter SO_2 emissions standards in China. Proc. Natl. Acad. Sci. U. S. A 115 (27), 7004. https://doi.org/10.1073/pnas.1800605115.

Krotkov, N.A., McLinden, C.A., Li, C., Lamsal, L.N., Celarier, E.A., Marchenko, S.V., Swartz, W.H., Bucsela, E.J., Joiner, J., Duncan, B.N., Boersma, K.F., Veefkind, J.P., Levelt, P.F., Fioletov, V.E., Dickerson, R.R., He, H., Lu, Z.F., Streets, D.G., 2016. Aura OMI observations of regional SO_2 and NO_2 pollution changes from 2005 to 2015. Atmos. Chem. Phys. 16 (7), 4605–4629. https://doi.org/10.5194/acp-16-4605-2016.

Li, J.C., Gao, Q.X., Li, L., Zheng, Y.F., Gao, W.K., 2018. Enlightenment and suggestions on the air quality of Beijing, Tianjin and Hebei revealed by primary pollutants. Res. Environ. Sci. 31 (10), 1651–1661. https://doi.org/10.13198/j.issn.1001-6929.2018.07.07 (In Chinese).

Li, K., Jacob, D.J., Liao, H., Shen, L., Zhang, Q., Bates, K.H., 2019. Anthropogenic drivers of 2013–2017 trends in summer surface ozone in China. Proc. Natl. Acad. Sci. U. S. A 116 (2), 422. https://doi.org/10.1073/pnas.1812168116.

Li, R., Fu, H.B., Cui, L.L., Li, J.L., Wu, Y., Meng, Y., Wang, Y.T., Chen, J.M., 2019. The spatiotemporal variation and key factors of SO_2 in 336 cities across China. J. Clean. Prod. 210, 602–611. https://doi.org/10.1016/j.jclepro.2018.11.062.

Li, X.Y., Wagner, F., Peng, W., Yang, J.N., Mauzerall, D.L., 2017. Reduction of solar photovoltaic resources due to air pollution in China. Proc. Natl. Acad. Sci. U. S. A 114 (45), 11867–11872. https://doi.org/10.1073/pnas.1711462114.

Li, Y.J., Sun, Y.L., Zhang, Q., Li, X., Li, M., Zhou, Z., Chan, C.K., 2017. Real-time chemical characterization of atmospheric particulate matter in China: a review. Atmos. Environ. 158, 270–304. https://doi.org/10.1016/j.atmosenv.2017.02.027.

Liang, P.F., Zhu, T., Fang, Y.H., Li, Y.R., Han, Y.Q., Wu, Y.S., Hu, M., Wang, J.X., 2017. The role of meteorological conditions and pollution control strategies in reducing air pollution in Beijing during APEC 2014 and Victory Parade 2015. Atmos. Chem. Phys. 17 (22), 13921–13940. https://doi.org/10.5194/acp-17-13921-2017.

Lin, C.Q., Liu, G., Lau, A.K.H., Li, Y., Li, C.C., Fung, J.C.H., Lao, X.Q., 2018. High-resolution satellite remote sensing of provincial $PM_{2.5}$ trends in China from 2001 to 2015. Atmos. Environ. 180, 110–116. https://doi.org/10.1016/j.atmosenv.2018.02.045.

Liu, H.J., Tian, H.Z., Zhang, K., Liu, S.H., Cheng, K., Yin, S.S., Liu, Y.L., Liu, X.Y., Wu, Y.M., Liu, W., Bai, X.X., Wang, Y., Shao, P.Y., Luo, L.N., Lin, S.M., Chen, J., Liu, X.G., 2019. Seasonal variation, formation mechanisms and potential sources of $PM_{2.5}$ in two typical cities in the Central Plains Urban Agglomeration, China. Sci. Total Environ. 657, 657–670. https://doi.org/10.1016/j.scitotenv.2018.12.068.

Liu, M.X., Huang, X., Song, Y., Xu, T.T., Wang, S.X., Wu, Z.J., Hu, M., Zhang, L., Zhang, Q., Pan, Y.P., Liu, X.J., Zhu, T., 2018. Rapid SO_2 emission reductions significantly increase tropospheric ammonia concentrations over the North China Plain. Atmos. Chem. Phys. 18 (24), 17933–17943. https://doi.org/10.5194/acp-18-17933-2018.

Liu, Y., Zheng, M., Yu, M.Y., Cai, X.H., Du, H.Y., Li, J., Zhou, T., Yan, C.Q., Wang, X.S., Shi, Z.B., Harrison, R.M., Zhang, Q., He, K.B., 2019. High-time-resolution source apportionment of $PM_{2.5}$ in Beijing with multiple models. Atmos. Chem. Phys. 19 (9), 6595–6609. https://doi.org/10.5194/acp-19-6595-2019.

Luo, J.Q., Du, P.J., Samat, A., Xia, J.S., Che, M.Q., Xue, Z.H., 2017. Spatiotemporal pattern of $PM_{2.5}$ concentrations in mainland China and analysis of its influencing factors using geographically weighted regression. Sci. Rep. 7, 40607. https://doi.org/10.1038/srep40607.

Ma, M.D., Yan, R., Du, Y.J., Ma, X.R., Cai, W.G., Xu, P.P., 2017. A methodology to assess China's building energy savings at the national level: an IPAT–LMDI model approach. J. Clean. Prod. 143, 784–793.

Ma, Z.W., Hu, X.F., Sayer, A.M., Levy, R., Zhang, Q., Xue, Y.G., Tong, S.L., Bi, J., Huang, L., Liu, Y., 2015. Satellite-based Spatiotemporal Trends in $PM_{2.5}$ Concentrations: China, 2004-2013. Environmental Health Perspectives.

National Bureau of Statistics of China (NBS), 2014. China Statistical Yearbook. China Statistics Press, Beijing, China, 2013 (in Chinese).

Pei, L., Yan, Z.W., 2018. Diminishing clear winter skies in Beijing towards a possible future. Environ. Res. Lett. 13 (12), 124029. https://doi.org/10.1088/1748-9326/aaf032.

Ren, Y.Q., Li, H., Meng, F., Wang, G.H., Zhang, H., Yang, T., Li, W.J., Ji, Y.Y., Bi, F., Wang, X.Z., 2019. Impact of emission controls on air quality in Beijing during the 2015 China Victory Day Parade: implication from organic aerosols. Atmos. Environ. 198, 207–214. https://doi.org/10.1016/j.atmosenv.2018.10.061.

Requia, W.J., Adams, M.D., Arain, A., Papatheodorou, S., Koutrakis, P., Mahmoud, M., 2017. Global association of air pollution and cardiorespiratory diseases: a systematic review, meta-analysis, and investigation of modifier variables. Am. J. Public Health 108 (S2), S123–S130. https://doi.org/10.2105/AJPH.2017.303839.

Rosenfeld, D., Zhu, Y.N., Wang, M.H., Zheng, Y.T., Goren, T., Yu, S.C., 2019. Aerosol-driven droplet concentrations dominate coverage and water of oceanic low-level clouds. Science 363 (6427), eaav0566. https://doi.org/10.1126/science.aav0566.

Shao, P.Y., Tian, H.Z., Sun, Y.J., Liu, H.J., Wu, B.B., Liu, S.H., Liu, X.Y., Wu, Y.M., Liang, W.Z., Wang, Y., Gao, J.J., Xue, Y.F., Bai, X.X., Liu, W., Lin, S.M., Hu, G.Z., 2018. Characterizing remarkable changes of severe haze events and chemical compositions in multi-size airborne particles (PM_1, $PM_{2.5}$ and PM_{10}) from January 2013 to 2016–2017 winter in Beijing, China. Atmos. Environ. 189, 133–144. https://doi.org/10.1016/j.atmosenv.2018.06.038.

Shen, Y., Zhang, L.P., Fang, X., Ji, H.Y., Li, X., Zhao, Z.W., 2019. Spatiotemporal patterns of recent $PM_{2.5}$ concentrations over typical urban agglomerations in China. Sci. Total Environ. 655, 13–26. https://doi.org/10.1016/j.scitotenv.2018.11.105.

Shi, P., Wu, M., Qu, S.M., Jiang, P., Qiao, X.Y., Chen, X., Zhou, M., Zhang, Z.C., 2015. Spatial distribution and temporal trends in precipitation concentration indices for the Southwest China. Water Resour. Manag. 29 (11), 3941–3955. https://doi.org/10.1007/s11269-015-1038-3.

Shi, X.Q., Zhao, C.F., Jiang, J.H., Wang, C.Y., Yang, X., Yung, Y.L., 2018. Spatial representativeness of $PM_{2.5}$ concentrations obtained using observations from network stations. J. Geophys. Res.: Atmosphere 123 (6), 3145–3158. https://doi.org/10.1002/2017jd027913.

Silver, B., Reddington, C.L., Arnold, S.R., Spracklen, D.V., 2018. Substantial changes in air pollution across China during 2015–2017. Environ. Res. Lett. 13 (11), 114012. https://doi.org/10.1088/1748-9326/aae718.

Song, J., Lu, M.X., Lu, J.G., Chao, L., An, Z., Liu, Y., Xu, D.Q., Wu, W.D., 2019. Acute effect of ambient air pollution on hospitalization in patients with hypertension: a time-series study in Shijiazhuang, China. Ecotoxicol. Environ. Saf. 170, 286–292. https://doi.org/10.1016/j.ecoenv.2018.11.125.

Sun, Y.L., Wang, Z.F., Wild, O., Xu, W.Q., Chen, C., Fu, P.Q., Du, W., Zhou, L.B., Zhang, Q., Han, T.T., Wang, Q.Q., Pan, X.L., Zheng, H.T., Li, J., Guo, X.F., Liu, J.G., Worsnop, D.R., 2016. APEC Blue": secondary aerosol reductions from emission controls in Beijing. Sci. Rep. 6, 20668. https://doi.org/10.1038/srep20668.

Tian, Y.L., Jiang, Y., Liu, Q., Xu, D.X., Zhao, S.D., He, L.H., Liu, H.J., Xu, H., 2019. Temporal and spatial trends in air quality in Beijing. Landsc. Urban Plan. 185, 35–43. https://doi.org/10.1016/j.landurbplan.2019.01.006.

Tie, X.X., Huang, R.J., Dai, W.T., Cao, J.J., Long, X., Su, X.L., Zhao, S.Y., Wang, Q.Y., Li, G.H., 2016. Effect of heavy haze and aerosol pollution on rice and wheat productions in China. Sci. Rep. 6, 29612. https://doi.org/10.1038/srep29612.

Wang, T., Wang, P.C., Theys, N., Tong, D., Hendrick, F., Zhang, Q., Van Roozendael, M., 2018. Spatial and temporal changes in SO_2 regimes over China in the recent decade and the driving mechanism. Atmos. Chem. Phys. 18 (24), 18063–18078. https://doi.org/10.5194/acp-18-18063-2018.

Wang, X.Y., Dickinson, R.E., Su, L.Y., Zhou, C.L., Wang, K.C., 2018. $PM_{2.5}$ pollution in China and how it has been exacerbated by terrain and meteorological conditions. Bull. Am. Meteorol. Soc. 99 (1), 105–119. https://doi.org/10.1175/bams-d-16-0301.1.

Xia, Y., Guan, D.B., Jiang, X.J., Peng, L.Q., Schroeder, H., Zhang, Q., 2016. Assessment of socioeconomic costs to China's air pollution. Atmos. Environ. 139, 147–156. https://doi.org/10.1016/j.atmosenv.2016.05.036.

Xu, Y.L., Xue, W.B., Lei, Y., Zhao, Y., Cheng, S.Y., Ren, Z.H., Huang, Q., 2018. Impact of meteorological conditions on $PM_{2.5}$ pollution in China during winter. Atmosphere 9 (11), 429. https://doi.org/10.3390/atmos9110429.

Yan, D., Lei, Y.L., Shi, Y.K., Zhu, Q., Li, L., Zhang, Z.E., 2018. Evolution of the spatiotemporal pattern of $PM_{2.5}$ concentrations in China – a case study from the Beijing-Tianjin-Hebei region. Atmos. Environ. 183, 225–233. https://doi.org/10.1016/j.atmosenv.2018.03.041.

Yuan, T.G., Chen, S.Y., Huang, J.P., Wu, D.Y., Lu, H., Zhang, G.L., Ma, X.J., Chen, Z.Q., Luo, Y., Ma, X.H., 2019. Influence of dynamic and thermal forcing on the meridional transport of Taklimakan Desert dust in spring and summer. J. Clim. 32 (3), 749–767. https://doi.org/10.1175/jcli-d-18-0361.1.

Zhang, K.Y., Zhao, C.F., Fan, H., Yang, Y.K., Sun, Y., 2019. Toward understanding the differences of $PM_{2.5}$ characteristics among five China urban cities. Asia-Pacific J. Atmos. Sci. https://doi.org/10.1007/s13143-019-00125-w.

Zhang, X.Y., Xu, X.D., Ding, Y.H., Liu, Y.J., Zhang, H.D., Wang, Y.Q., Zhong, J.T., 2019. The impact of meteorological changes from 2013 to 2017 on $PM_{2.5}$ mass reduction in key regions in China. Sci. China Earth Sci. 62 https://doi.org/10.1007/s11430-019-9343-3.

Zhang, Z.Y., Zhang, X., Gong, D.Y., Kim, S.J., Mao, R., Zhao, X., 2016. Possible influence of atmospheric circulations on winter haze pollution in the Beijing–Tianjin–Hebei region, northern China. Atmos. Chem. Phys. 16 (2), 561–571. https://doi.org/10.5194/acp-16-561-2016.

Zhao, C.F., Lin, Y.L., Wu, F., Wang, Y., Li, Z.Q., Rosenfeld, D., Wang, Y., 2018. Enlarging rainfall area of tropical cyclones by atmospheric aerosols. Geophys. Res. Lett. https://doi.org/10.1029/2018GL079427.

Zhao, C.F., Wang, Y., Shi, X.Q., Zhang, D.Z., Wang, C.Y., Jiang, J.H., Zhang, Q., Fan, H., 2019. Estimating the contribution of local primary emissions to particulate pollution using high-density station observations. J. Geophys. Res.: Atmosphere 124 (3), 1648–1661. https://doi.org/10.1029/2018jd028888.

Zheng, C.W., Zhao, C.F., Li, Y.P., Wu, X.L., Zhang, K.Y., Gao, J., Qiao, Q., Ren, Y.Z., Zhang, X., Chai, F.H., 2018. Spatial and temporal distribution of NO_2 and SO_2 in Inner Mongolia urban agglomeration obtained from satellite remote sensing and ground observations. Atmos. Environ. 188, 50–59. https://doi.org/10.1016/j.atmosenv.2018.06.029.

Zhong, S., Qian, Y., Sarangi, C., Zhao, C., Leung, R., Wang, H.L., Yan, H.P., Yang, T., Yang, B., 2018. Urbanization effect on winter haze in the Yangtze River delta region of China. Geophys. Res. Lett. 45 https://doi.org/10.1029/2018GL077239.

Zhou, Y.J., Zhou, J.X., 2017. Urban atmospheric environmental capacity and atmospheric environmental carrying capacity constrained by GDP–$PM_{2.5}$. Ecol. Indicat. 73, 637–652. https://doi.org/10.1016/j.ecolind.2016.10.015.